REPORT

# Resilience of the temperate coral *Oculina arbuscula* to ocean acidification extends to the physiological level

Cydney Wang[1] · Erin M. Arneson[2] · Daniel F. Gleason[2] · Brian M. Hopkinson[1]

**Abstract** Both juvenile and adult life stages of the temperate scleractinian coral *Oculina arbuscula* are resilient to the effects of moderate ocean acidification (OA) in contrast to many tropical corals in which growth and calcification rates are suppressed. Here, potential mechanisms of resilience to OA related to photosynthetic physiology and inorganic carbon processing were studied in adult *O. arbuscula* colonies. After exposing colonies to ambient and elevated carbon dioxide ($CO_2$) treatments for 7 weeks, photosynthetic performance was characterized using photosynthesis versus irradiance experiments, chlorophyll fluorescence kinetics, and algal pigment content. Inorganic carbon-processing capabilities were assessed by measurement of internal and external carbonic anhydrase activity of the coral host, internal carbonic anhydrase activity of symbiotic algae, and the reliance of photosynthesis on external carbonic anhydrase. Photosynthetic physiology was unaffected by OA ruling out the possibility that resilience was mediated by increased photosynthetic energy supply. Carbonic anhydrase activities were maintained at elevated $CO_2$ suggesting no major rearrangements of the inorganic carbon-processing machinery, but this could be a sign of resilience since tropical corals often down-regulate carbonic anhydrases at high $CO_2$. The general lack of effect of ocean acidification on these physiological traits suggests other characteristics, such as maintenance of calcifying fluid pH and ability to acquire energy from heterotrophy, may be more important for the resilience of *O. arbuscula* to OA.

**Keywords** Ocean acidification · Coral · Resilience · Physiology · Oculina

Topic Editor Anastazia Teresa Banaszak

✉ Brian M. Hopkinson
bmhopkin@uga.edu

1 Department of Marine Sciences, University of Georgia, Athens, GA 30602, USA

2 James H. Oliver, Jr., Institute for Coastal Plain Science, Georgia Southern University, Statesboro, GA 30460-8042, USA

## Introduction

The oceans absorb approximately 30% of the carbon dioxide ($CO_2$) released by anthropogenic activities such as fossil fuel burning and land use change (Gruber et al. 2019). Absorption of $CO_2$ creates carbonic acid ($H_2CO_3$) causing a decrease in the pH of seawater and numerous associated chemical changes collectively referred to as ocean acidification (OA) (Doney et al. 2009). Most notable among these changes are decreased carbonate ion ($CO_3^{2-}$) concentrations and increased bicarbonate ($HCO_3^-$) concentrations, which are consequences of re-equilibration of the carbonate buffer system after $CO_2$ absorption. OA affects marine organisms, populations, and ecosystems in diverse but often subtle ways (Hofmann et al. 2010; Kroeker et al. 2013). Photosynthetic organisms such as algae and seagrasses often benefit from increased $CO_2$ concentrations that either directly or indirectly stimulate photosynthesis (Koch et al. 2013; Mackey et al. 2015). The relative benefit of OA for photosynthetic performance accrues differentially to community members leading to shifts in the relative species abundance (Tortell et al. 2008).

While OA may benefit certain photoautotrophs, it is generally detrimental to the many marine organisms that make calcium carbonate skeletons or shells. OA reduces the rate of calcification in many corals, mollusks, and other marine calcifiers (Riebesell et al. 2000; Ries et al. 2009; Kroeker et al. 2010). However, the mechanism by which OA inhibits calcification has not been definitively identified and likely varies between taxa. OA causes a reduction in carbonate concentrations, the form of inorganic carbon ultimately required to make calcium carbonate minerals, but many calcifiers can make use of bicarbonate as well as carbonate by carefully controlling fluid chemistry in the spaces where calcium carbonate is deposited (Tambutte et al. 2011; Drake et al. 2020). This ability to use more than one inorganic carbon source implies that the physiological consequences of OA that lead to reduced calcification rates are more complex than simple lack of substrate (carbonate) availability (Comeau et al. 2013). This complexity is most evident in the few unusual species that calcify more rapidly with OA, perhaps taking advantage of the increased bicarbonate concentration (Ries et al. 2009).

Scleractinian corals have received substantial attention regarding OA given their ecological importance as reef builders and the current pressures from thermal bleaching, diseases, overfishing, and eutrophication (Edmunds et al. 2016; Zaneveld et al. 2016; Hughes et al. 2018; Muller et al. 2020). Calcification in corals is a highly regulated process, and the mechanism by which OA impacts corals is not yet fully understood. Corals deposit calcium carbonate from the calcifying fluid, a thin layer of fluid generated between the coral's innermost tissue layer and existing skeleton (Cohen and McConnaughey 2003; Tambutte et al. 2011). Active proton export from the calcifying fluid increases its pH (typically pH 8–9) converting inorganic carbon into carbonate, thereby raising the calcium carbonate saturation state to maintain calcification (Sevilgen et al. 2019). Inorganic carbon is delivered to the calcifying fluid to support calcification, and this inorganic carbon is ultimately derived from a mix of respiratory $CO_2$ and inorganic carbon imported from seawater (Furla et al. 2000). Delivery of inorganic carbon to the calcifying fluid is facilitated by the enzyme carbonic anhydrase, which accelerates the interconversion of $CO_2$ and bicarbonate (Bertucci et al. 2013). Carbonic anhydrase is involved in $CO_2$ uptake by corals (Tansik et al. 2015), routing of inorganic carbon through coral tissues layers (Bertucci et al. 2013), and calcification (Moya et al. 2008).

Given the complexity of calcification, it has been challenging to identify the critical processes negatively affected by OA. One key piece of evidence is that OA reduces the pH of the calcifying fluid in scleractinian corals, which lowers the aragonite saturation state and slows calcification rates in some species (e.g., *Stylophora pistillata*, *Acropora*

*yongei*), while others are more resilient (e.g., *Pocillopora damicornis*) (Venn et al. 2013; Comeau et al. 2018). How OA decreases calcifying fluid pH is an open question, but one hypothesis is that increased $CO_2$ concentrations in the water drive increased $CO_2$ fluxes to the calcifying fluid, acidifying the calcifying fluid in a manner analogous to that by which absorption of anthropogenic $CO_2$ acidifies seawater (Cai et al. 2016).

The relative impact of OA on calcification of scleractinian corals seems to be modulated by species, growth characteristics, and environmental factors (Chan and Connolly 2013; Comeau et al. 2014). The coral host could theoretically benefit from the increased photosynthetic potential that elevated seawater $CO_2$ concentrations offer to their symbiotic algae. Generation of additional photosynthetic energy could be used to compensate for the otherwise detrimental effect of OA on calcification. Though there have been sporadic reports of stimulation of photosynthesis by OA (Langdon and Atkinson 2005), the symbiotic algae of most coral species are impacted neither positively nor negatively (Anthony et al. 2008; Hoadley et al. 2015).

Although tropical coral growth is commonly slowed by near future ($\sim$ year 2100) levels of OA, many subtropical and temperate corals, including *Oculina arbuscula*, are more resilient to this stress (Ries et al. 2010; Rodolfo-Metalpa et al. 2010; Varnerin et al. 2020). *Oculina arbuscula* is a common branching scleractinian coral found in subtropical to temperate hard bottom habitats along the southeastern coast of the USA (Gleason et al. 2018). It is facultatively symbiotic with dinoflagellates from the family Symbiodiniaceae, most commonly associating with *Brevolium psygmophilum* (Thornhill et al. 2008; Leydet and Hellberg 2016; LaJeunesse et al. 2018), with colonies from well-lit environments generally hosting abundant symbionts and colonies from darker habitats having fewer to no symbionts and instead relying on heterotrophy. Unlike tropical corals, *O. arbuscula* in shallow water habitats (< 30 m depth) of the southeastern USA are often exposed to highly seasonal environments where temperatures and $CO_2$ concentrations vary greatly throughout the year (Stachowicz and Hay 1999; Xue et al. 2016). Perhaps in part due to the natural variability in $CO_2$, calcification rates of adults and juveniles of this species are resilient to OA (Ries et al. 2010; Varnerin et al. 2020). Juveniles were only modestly affected by $CO_2$ concentrations similar to predicted year 2100 concentrations (1300 ppm; Varnerin et al. 2020), conditions that substantially inhibit calcification in many tropical corals (Comeau et al. 2014; Langdon et al. 2018). Adults were similarly resilient until $CO_2$ concentrations reached $\sim$ 3000 ppm when calcification was dramatically reduced (Ries et al. 2010).

While it is clear that growth and calcification of *O. arbuscula* are relatively unaffected by OA, the mechanisms behind this resilience, including any compensating physiological adjustments, have not been examined. Here, we sought to assess the effects of OA on components of the inorganic carbon delivery system, carbonic anhydrases, and photosynthetic physiology. We hypothesized that adjustments to the inorganic carbon delivery processes induced by OA could mitigate its detrimental effects or allow reallocation of resources to other processes that could maintain calcification, such as proton export from the calcifying fluid (McCulloch et al. 2012). As an alternate potential response, we hypothesized that the photosynthetic system may acclimate to take advantage of increased $CO_2$ availability, enhancing photosynthetic energy generation that could be used to mitigate detrimental effects of OA on the calcification process.

## Materials and methods

### Coral collection and experimental design

A total of 22, 6–10-cm-long fragments of *O. arbuscula* were collected on May 23, 2018, at approx. 20 m depth at J–Y Reef (31° 36.056, 80° 47.431), a relict scallop shell reef located off the coast of Georgia, USA. At the time of collection, daily average water temperature was 24.6 ± 0.3 C and seawater $pCO_2$ was 524 ± 6 ppm at the nearby Gray's Reef Buoy (https://www.ndbc.noaa.gov/station_page.php?station=41008). Care was taken to sample from coral colonies that were consistently brown in color with no visible signs of bleaching and that were separated by ≥ 1 m so that they were more likely to be genetically distinct. Coral fragments were removed from larger colonies using a chisel and rock hammer. *Oculina arbuscula* fragments were transported in insulated coolers inside temperature-controlled vehicles to the laboratory at Georgia Southern University (Statesboro, GA) in seawater collected from the reef. The coral fragments were left in the cooler with the lid open and with aeration for the next 24 h to allow the sea water to cool down to the room temperature of 23 °C. Following their initial 24-h temperature acclimation, each colony fragment was mounted to a 4.7 × 4.7 cm ceramic tile using underwater epoxy (Z-Spar A-788 Splash Zone Compound). Fragments and their attached ceramic tiles were held at 23 °C in 38-L aquaria containing artificial seawater (Instant Ocean) until they were transported to the University of Georgia (Athens, GA) 9 days later where OA experiments were conducted. At the University of Georgia, corals were again allowed to acclimate to new tank conditions (detailed below) for 1 week prior to beginning $CO_2$ manipulation.

The OA experiment consisted of two treatments, ambient and elevated $CO_2$, with three replicate tanks per treatment. To allocate the 22 coral fragments among treatments, the corals were paired by mass (30–95 g) and one member of each pair was assigned to each treatment to ensure the size of corals was similar between treatments. The corals were then randomly assigned to tanks within treatments. Tanks (38 L) were filled with artificial seawater (Red Sea 'Red Sea Salt Mix') made up in deionized water at a salinity of 35 psu. Prior to addition to the tanks, elevated alkalinity concentrations in the artificial seawater were reduced to 2.4 mM using HCl. Temperature was maintained between 25 and 27 °C. Aquarium water was continuously filtered through physical and charcoal filters. Ambient $CO_2$ treatments were bubbled with laboratory air (∼ 420 ppm $CO_2$) using aquarium air pumps through a fritted air stone to increase gas exchange rates. Elevated $CO_2$ treatments were bubbled with high $CO_2$ air (1000 ppm $CO_2$) through a fritted air stone. High $CO_2$ air was obtained by mixing laboratory air with pure $CO_2$ using mass flow controllers (Aalborg), and the $CO_2$ content was verified using an infrared gas analyzer (LiCor LI-840A). The seawater inorganic carbon system in each tank was monitored routinely by measuring pH (3 times per week) and alkalinity (at minimum weekly). pH was measured on the total hydrogen ion scale using the thymol blue spectrophotometric method (Zhang and Byrne 1996). Alkalinity was measured by an open-cell Gran titration (Dickson and Goyet 1994) using an automated titrator (Apollo SciTech ALK1+) that was calibrated with certified reference material (Reference material for oceanic $CO_2$ measurements, Scripps Institution of Oceanography, Batch 132). $CO_2$ levels in the tanks generally matched target conditions (Table 1, Supplementary Figure 1) with ambient $CO_2$ concentrations approximating the elevated summertime $pCO_2$ conditions at Gray's Reef (∼ 400–500 ppm; Xue et al. 2016) and high $CO_2$ treatments of approximately 840 ppm, consistent with business as usual scenarios for year 2100 (Riebesell et al. 2011; IPCC 2014). Alkalinity in the tanks (2.3–2.36 mM; Table 1; Supplementary

**Table 1** Tank inorganic carbon chemistry averaged over the course of the experiment

| Parameter | Ambient | High $CO_2$ |
|---|---|---|
| Alkalinity (mM) | 2.31 ± 0.20 | 2.37 ± 0.17 |
| $pH_T$ | 7.97 ± 0.08 | 7.78 ± 0.09 |
| $pCO_2$ (ppm) | 490 ± 106 | 840 ± 186 |
| Bicarbonate (mM) | 1.85 ± 0.14 | 2.05 ± 0.13 |
| Carbonate (μM) | 201 ± 34 | 138 ± 23 |

Standard deviations represent variability over time within treatments

Figure 1) was also consistent with spring to summertime concentrations at Gray's Reef (2.3–2.4 mM; Xue et al. 2016).

The aquariums were illuminated with LED lights at 40–60 μmol photons $m^{-2} s^{-1}$ for 12 h per day, similar to conditions in Georgia hard bottom environments (40–155 μmol photons $m^{-2} s^{-1}$; Matterson 2012). Corals were fed with freshly hatched *Artemia* sp. nauplii ad libitum three times per week for 2 h. Feeding was conducted in an isolated tray within the aquarium, and any uneaten nauplii were removed from the aquarium after feeding. Partial water changes (~ 25%) and tank cleanings were conducted once a week.

### Coral and algal symbiont biometrics

Coral calcification rates were measured using the change in buoyant weight over the course of the 7-week experiment (Jokiel et al. 1978). At the beginning and end of the experiment, each coral fragment was suspended from a monofilament line attached to its base on the underhook of an analytical balance. The coral fragments were immersed in aquarium water during the measurement, and weights were recorded to the nearest milligram. At the end of the experiment, coral tissue was removed using either a water-pik or airbrush filled with artificial seawater depending on whether carbonic anhydrase activities were measured on the fragment. Airbrushing produces a more concentrated suspension needed for carbonic anhydrase measurements (described below). The resulting coral–algal slurry was homogenized, and algae were removed from the homogenate via centrifugation at 2350 g for 5 min. Fragment surface area was measured in duplicate from the weight of aluminum foil wrapped around the fragment (Marsh 1970). A calibration curve was generated by weighting foil pieces of known size to convert foil weight to coral surface area.

Algal symbiont cell density and pigment content were determined from the centrifuged coral homogenate. The resulting algal pellet was resuspended in artificial seawater, and a fraction was preserved with formalin (1%) for cell density estimation. Algal cells in the preserved fraction were enumerated (three times) using a hemacytometer, and cell densities were normalized to coral surface area. A systematic downward bias in algal cell densities was observed in corals from which tissue had been removed using an airbrush as opposed to a water-pik. The magnitude of this bias was estimated by dividing the average cell densities in all water-piked corals by the average cell densities in all airbrushed corals. This bias factor (2.2 ± 1.3) was used to scale up algal cell densities in airbrushed corals. The source of this bias is suspected to be clumping of algae in the airbrushed coral samples, clumps that were then not included in the hemacytometer cell. We

verified that effectively all algae were pelleted in the centrifugation procedure and there were no biases in other parameters. Most notably there was no evident bias in algal pigment concentrations per unit coral surface area in air-brushed versus water-piked samples, which would indicate loss of algae at some point or incomplete tissue removal in the airbrushed samples.

Algal pigment concentrations were determined via Gaussian curve fitting to UV/Vis absorption spectra of pigment extracts. A portion of the coral–algal homogenate obtained via airbrushing or water-piking was centrifuged (2350 g, 5 min), and the algal pellet was stored at − 20 °C for less than 1 week. To extract pigments, a 90% acetone–10% water solution was added to the algal pellet and sonicated with a probe sonicator for 1 min to disrupt algal aggregates. The solution was allowed to extract for 48 h at − 20 °C. The extract was clarified by brief centrifugation, and then the UV/Vis absorption spectrum was measured from 350 to 750 nm. The concentrations of selected pigments were determined by nonlinear least squares fitting of Gaussian components to the absorption spectrum (400–700 nm) using the method described in Thrane et al. (2015). Pigments known to be found in dinoflagellates (chlorophyll *a*, chlorophyll *c*2, peridinin, beta-carotene, dinoxanthin, diatoxanthin, and diadinoxanthin) were included in the fitting procedure using reference spectra supplied by Thrane et al. (2015). The dominant pigments were determined to be chlorophyll *a*, chlorophyll *c*2, and peridinin whose concentrations are reported.

### Carbonic anhydrase activity

Internal and external carbonic anhydrase (iCA and eCA, respectively) activities were measured in corals, and iCA activity was measured in algal symbionts using $^{18}O$ exchange methods. eCA activity includes any CA exposed to the environment on the outer surface of polyps or coenosarc tissue. Coral iCA activity includes any CA within the tissues, mesoglea, or calcifying fluid, and symbiont iCA activity includes any CA within the algal symbionts regardless of localization (cytoplasm, chloroplast, etc.). Due to time constraints, only a subset of the coral fragments (coral eCA: 8 per treatment, coral iCA: 6 per treatment, symbiont iCA: 6 per treatment) were assayed for CA activity. CA activities were determined based on the rate of removal of an $^{18}O$-label from DIC, monitored via membrane inlet mass spectrometry (MIMS). As $CO_2$ is hydrated and bicarbonate-dehydrated, the $^{18}O$-label is gradually exchanged for $^{16}O$ from water; CA accelerates the hydration/dehydration reaction and so accelerates removal of the $^{18}O$-label (Silverman 1982).

Coral eCA activity was measured on intact coral fragments as detailed in Tansik et al. (2015). The

measurements were conducted in a water-jacketed (26 °C), stirred chamber filled with pH-buffered, artificial seawater (Red Sea Salt Mix, pH = 8.0, 10 mM Bicine buffer) from which water was continuously removed at a rate of ~ 500 μL min$^{-1}$ using a peristaltic pump. The water was passed through a flow-through MIMS inlet, which consisted of a 25 mm length of gas-permeable silicone tubing under high vacuum, to extract gases including $CO_2$. The extracted gas passed through a dry ice/ethanol water trap (− 75 °C) and into a mass spectrometer (Pfeiffer PrismaPlus QMS220), which continuously monitored isotopologues of $CO_2$. To initiate the experiment, $^{18}$O–$^{13}$C-labeled DIC (100 μM) was added to the chamber and the background rate of $^{18}$O exchange was monitored for ~ 20 min. A coral fragment was then added to the chamber, and any acceleration of $^{18}$O removal was monitored for ~ 25 min at which point an eCA inhibitor, acetazolamide (50 μM), was added to the chamber and $^{18}$O exchange was monitored for a further ~ 25 min. In the absence of the eCA inhibitor, accelerated $^{18}$O exchange is due to both eCA and iCA, whereas after the application of the inhibitor accelerated $^{18}$O exchange is only due to iCA. The $^{18}$O exchange data were analyzed to determine eCA activity by fitting a numerical model to the data as detailed in Tansik et al. (2015). The first-order rate constant for $CO_2$ hydration (units of cm$^3$ s$^{-1}$), determined from the model–data fit, was normalized by coral surface area to provide an estimate of eCA activity per unit surface area (units of cm s$^{-1}$).

Coral iCA activity was measured on homogenized coral tissue subtracting the contribution of coral eCA as detailed in Hopkinson et al. (2015). To obtain a concentrated coral homogenate necessary for this assay, coral tissue was removed using an airbrush filled with assay buffer [DIC-free artificial seawater (Price et al. 1988) buffered to pH 8.0 using 20 mM TRIS] to which a protease inhibitor cocktail (Roche cOmplete protease inhibitor, 3 mini tablets per 50 mL) was added. The algal–coral slurry was homogenized and then centrifuged (2350 g, 5 min) to pellet symbiotic algae to produce a purified coral tissue homogenate. The CA activity of this purified homogenate was measured using an $^{18}$O removal technique. The mass spectrometer described above was interfaced to a small, water-jacketed (26 °C) chamber that holds ~ 1 mL of solution and has a Teflon membrane on the bottom through which gases can diffuse into the mass spectrometer. This chamber was filled with 800 μL assay buffer, and 2 mM $^{18}$O–$^{13}$C-labeled DIC was added to the chamber. After monitoring background $^{18}$O-exchange for ~ 10 min, 200 μL of the purified coral homogenate was added to the chamber and accelerated $^{18}$O-exchange was monitored for ~ 10 min at which point a CA inhibitor (50 μM acetazolamide) was added. Coral iCA activity was determined by fitting a numerical model to the $^{18}$O-exchange data as detailed in Hopkinson et al.

(2015). The first-order rate constant for $CO_2$ hydration (units of cm$^3$ s$^{-1}$), determined from the model–data fit, was normalized by coral surface area to provide an estimate of iCA activity per unit surface area (units of cm s$^{-1}$).

Algal symbiont iCA activity was measured on algae pelleted from the airbrushed corals and resuspended in assay buffer following Hopkinson et al. (2011). The procedure for algal iCA activity is similar to that described for the coral iCA except that 200 μL of algal suspension was added to the MIMS chamber instead of coral homogenate and the assay buffer contained 50 μM acetazolamide to inhibit eCA or any residual coral tissue CA activity. Algal symbiont iCA activity was determined by fitting a numerical model to the $^{18}$O-exchange data as detailed in Hopkinson et al. (2011). The first-order rate constant for $CO_2$ hydration (units of cm$^3$ s$^{-1}$), determined from the model–data fit, was normalized by algal cell volume resulting in units of s$^{-1}$ and providing an estimate of the CA activity, assuming that it is homogenously distributed throughout the cell (Hopkinson et al. 2011). The MATLAB code used to determine coral iCA and eCA and algal iCA is available at: https://github.com/bmhopkinson/18O_processing.

## Photosynthetic rates and physiology

Photosynthetic rates as a function of irradiance were determined on coral holobionts (coral + algal symbionts) by measuring $O_2$ production rates in metabolic chambers. Coral fragments were placed on a fritted base in a water-jacketed (26 °C) acrylic chamber containing artificial seawater whose pH was adjusted to match experimental conditions (ambient: 7.96 ± 0.02; high $CO_2$: 7.75 ± 0.02; Table 1). The chamber was stirred using a magnetic stir bar at 500 rpm, and oxygen was continuously monitored in the chamber using a calibrated Firesting oxygen optode. Irradiance was controlled by a LED light source (Cool-White 5000 K Cree) calibrated for the chamber using a Walz PAR meter. Irradiance was increased stepwise (0, 50, 100, 200, 300, 450, 650, and 900 μmol photons m$^{-2}$ s$^{-1}$) holding light levels constant for 8 min. P versus E data were fit to a saturating exponential function to extract the maximal gross photosynthetic rate ($P_{max}$), the light saturation parameter ($E_k$), and the dark respiration rate (R), which were subsequently normalized to specimen surface areas calculated as described above.

To determine the role of eCA in photosynthesis, experiments were conducted in which an eCA inhibitor (acetazolamide) was added to corals while they were photosynthesizing. To conduct these experiments, a coral fragment was placed in the same apparatus used to conduct photosynthesis versus irradiance experiments. Initially, oxygen depletion was monitored in the dark for 10 min to

constrain the respiration rate, at which point the LED lights were turned on to 600 µmol photons m$^{-2}$ s$^{-1}$ and the photosynthetic rate was monitored from oxygen production. After 10 min, 50 µM acetazolamide was added to the chamber and oxygen production was monitored for a further 10 min. Coral fragments were rinsed with seawater and returned to the tank and allowed to rest for at least 2 days before any other physiological experiments were performed.

Photosystem II (PSII) physiological parameters were determined using chlorophyll fluorescence saturation and relaxation kinetics. Chlorophyll fluorescence kinetics were measured at three locations on each coral fragment using a fiber-optic probe interfaced to a Satlantic FIRe chlorophyll fluorometer. During the single-turnover saturation phase, light (blue LED) was continuously applied for 200 µs, after which relaxation was monitored over 60 intervals with a base interval of 60 µs. During the multi-turnover saturation phase, light was applied continuously for 200 ms, after which relaxation was monitored over 40 intervals with a base interval of 100 µs. The single-turnover phase data were fit to the Kolber et al. (1998) model of chlorophyll fluorescence using a custom MATLAB script to calculate the initial fluorescence ($F_o$), the maximal fluorescence during the single-turnover phase ($F_m$), and the turnover time of $Q_A$ ($\tau_{QA}$). Variable fluorescence ($F_v$) was calculated as the difference between $F_m$ and $F_o$. A single exponential decay was fit to the multi-turnover relaxation phase data to determine the turnover time of the plastoquinone pool ($\tau_{PQ}$).

### Timing of measurements

After collection and acclimation, the experiment was deemed to have officially started when $CO_2$ conditions were manipulated, which was coincident with initial measurement of buoyant weights. After 7 full weeks of exposure to manipulated $CO_2$ conditions, measurements began with a final buoyant weight, then proceeded to nondestructive physiological measurements, and finally ended with destructive measurements over the course of 2 weeks. Of the nondestructive measurements, chlorophyll fluorescence kinetics were measured first in a single day, since this measurement is quick, and then followed by measurements of photosynthesis versus irradiance, coral eCA activity, and the effect of acetazolamide on photosynthesis. Other than chlorophyll fluorescence kinetics, these measurements were not conducted in a consistent order to facilitate throughput. However, care was taken to ensure coral fragments were allowed to rest for 2 days after exposure to acetazolamide. Finally, samples for destructive measurements were taken on each fragment simultaneously. These destructive measurements were: algal pigment content, algal symbiont density, and when taken coral iCA activity and algal symbiont iCA activity.

### Statistical analysis

For each variable, a nested ANOVA was conducted to assess the effect of the treatment ($CO_2$), accounting for any potential effect of individual tanks, which were nested within treatment. Because the experimental design was unbalanced (the number of corals in each tank varied), the analysis was conducted as a linear mixed effects model in R using the lme function from the nlme package. $CO_2$ treatment was specified as a fixed effect, and tank was specified as a random effect. The significance of the treatment effect for each variable is reported. The code and data are included in the Supplemental Materials.

### Results

The coral fragments appeared to maintain good health over the course of the experiment as evidenced by extension of polyps in the day, active feeding on *Artemia* sp., and lack of mortality or tissue loss. One coral in a high $CO_2$ treatment tank exhibited partial bleaching that began roughly half-way through the experiment and continued for the remainder of the experiment. This coral was removed from subsequent analyses. Over the course of the 7-week experiment, corals in both the ambient and high $CO_2$ treatments increased skeletal weight by $\sim$ 3% at an average rate of $0.52 \pm 0.10$ mg cm$^{-2}$ d$^{-1}$ and there was no significant difference in growth between the treatments (Fig. 1; Table 2). Algal symbiont density was
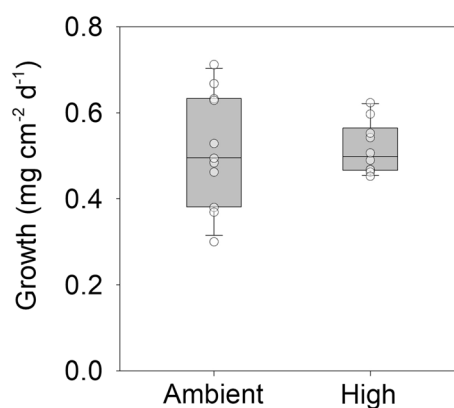


**Fig. 1** Skeletal growth at ambient (490 ppm) and high (840 ppm) $CO_2$ treatments. Skeletal growth rates were calculated from differences in buoyant weight from the beginning and end of the experiment. The lower and upper bounds of the boxes indicate the 25th and 75th percentiles of the data, and the extent of the whiskers indicates the 10th and 90th percentiles. The circles overlying the box plot are the individual data points (*n* per treatment = 9–11)

**Table 2** Results of nested one-way ANOVAs to assess differences in coral and algal biometrics between ambient and high $CO_2$ treatments ($n$ per treatment = 9–11)

| Variable | $F$ | $df$ | $p$ value |
|---|---|---|---|
| Growth | 0.001 | 1, 4 | 0.973 |
| Symbiont density | 0.18 | 1, 4 | 0.692 |
| Chl $a$ | 3.16 | 1, 4 | 0.150 |
| Chl $c2$ | 3.04 | 1, 4 | 0.156 |
| Peridinin | 2.50 | 1, 4 | 0.189 |

approximately $2 \times 10^6$ cells $cm^{-2}$ and was not significantly different between treatments (Fig. 2a; Table 2). It should be noted that the algal symbiont densities from coral fragments whose tissue was removed via airbrushing appeared to be underestimates, likely due to clumping, and consequently were corrected as detailed in the Materials and methods section. The dominant algal pigments detected were chlorophyll $a$ and peridinin, present at $\sim$ 1.25 pg cell$^{-1}$, and chlorophyll $c2$ present at $\sim$ 0.4 pg cell$^{-1}$ (Fig. 2b). Lower concentrations of beta-carotene and dinoxanthin were also detected. Average per cell pigment contents were not significantly affected by $CO_2$ treatment (Fig. 2b; Table 2).

The enzyme CA is involved in inorganic carbon processing for photosynthesis and calcification and is consequently one of the points at which OA may affect corals. Coral eCA and iCA activities were assessed as was algal iCA activity. Coral eCA activity was $\sim$ 1 cm s$^{-1}$ in most colonies and was not significantly different between $CO_2$ treatments (Fig. 3c; Table 3). The $^{18}$O-exchange model used to extract eCA activities generally fit the data well, indicating that the rates were accurately determined, and

there was a clear effect of the eCA inhibitor on $^{18}$O-exchange demonstrating that eCA was present (Fig. 3a). Coral iCA activity was 10–15 cm s$^{-1}$ and was not significantly different between treatments (Fig. 3d; Table 3). The model used to analyze the data fit well in most cases (Fig. 3b), but in one case biphasic depletion of $^{18}$O was observed. Biphasic depletion behavior is indicative of intact cells that contain CA in the homogenate, possibly due to incomplete breakage of coral cells or incomplete removal of algal symbionts. This sample was removed from the analysis. Algal symbiont iCA activities were very high, between 1000 and 2500 s$^{-1}$ (Fig. 3e), compared with activities of 20–500 s$^{-1}$ in diatoms (Hopkinson et al. 2011, 2013). There was no significant difference in algal symbiont iCA activity between treatments (Table 3).

OA can alter photosynthesis, and so photosynthetic physiology was characterized through photosynthesis versus irradiance experiments, chlorophyll fluorescence kinetics, and the effect of eCA inhibition on photosynthesis. Photosynthesis versus irradiance experiments showed that maximal photosynthetic rates were $\sim$ $4.5 \times 10^{-4}$ µmol cm$^{-2}$ s$^{-1}$, respiration rates averaged $\sim$ $1 \times 10^{-4}$ µmol cm$^{-2}$ s$^{-1}$, and $E_k$ was $\sim$ 225 µmol photons m$^{-2}$ s$^{-1}$ (Fig. 4). None of the photosynthesis versus irradiance parameters were significantly different between $CO_2$ treatments (Table 4). PSII characteristics, as assessed using chlorophyll fluorescence kinetics, were not affected by $CO_2$ treatments. $F_v/F_m$, a proxy for the maximal photosynthetic efficiency of PSII, was $\sim$ 0.4 in both treatments (Fig. 5a). The turnover time of the first electron acceptor in PSII ($\tau_{QA}$) was $\sim$ 1500 µs (Fig. 5b), and the turnover time of the plastoquinone pool ($\tau_{PQ}$) was $\sim$ 20 ms (Fig. 5c). Application of an inhibitor of eCA (acetazolamide) inhibited photosynthesis in nearly all coral fragments reducing
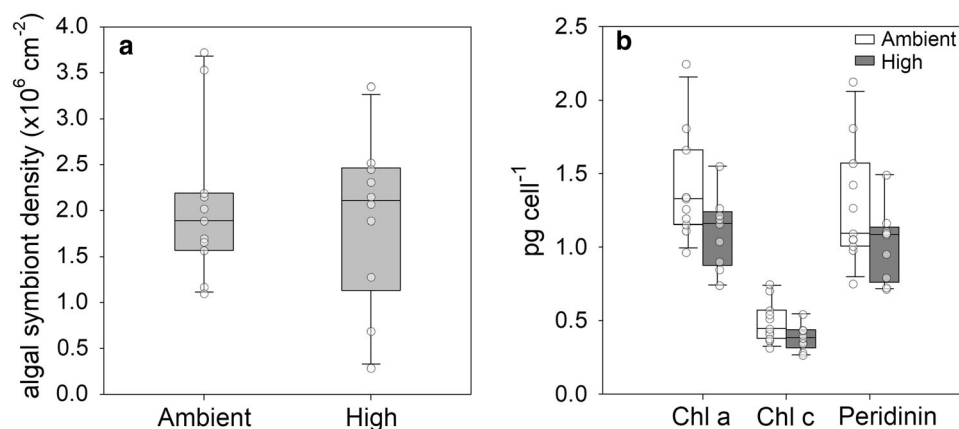


**Fig. 2** **a** Algal symbiont cell density and **b** algal pigment content for *O. arbuscula* in ambient (490 ppm) and high (840 ppm) $CO_2$ treatments. Algal symbiont densities were determined by direct microscopic count at the end of the experiment. Pigment content was determined by deconvolution of UV/Vis spectra of organic extracts obtained at the end of the experiment. The lower and upper bounds of the boxes indicate the 25th and 75th percentiles of the data, and the extent of the whiskers indicates the 10th and 90th percentiles. The circles overlying the box plot are the individual data points ($n$ per treatment = 9–11)
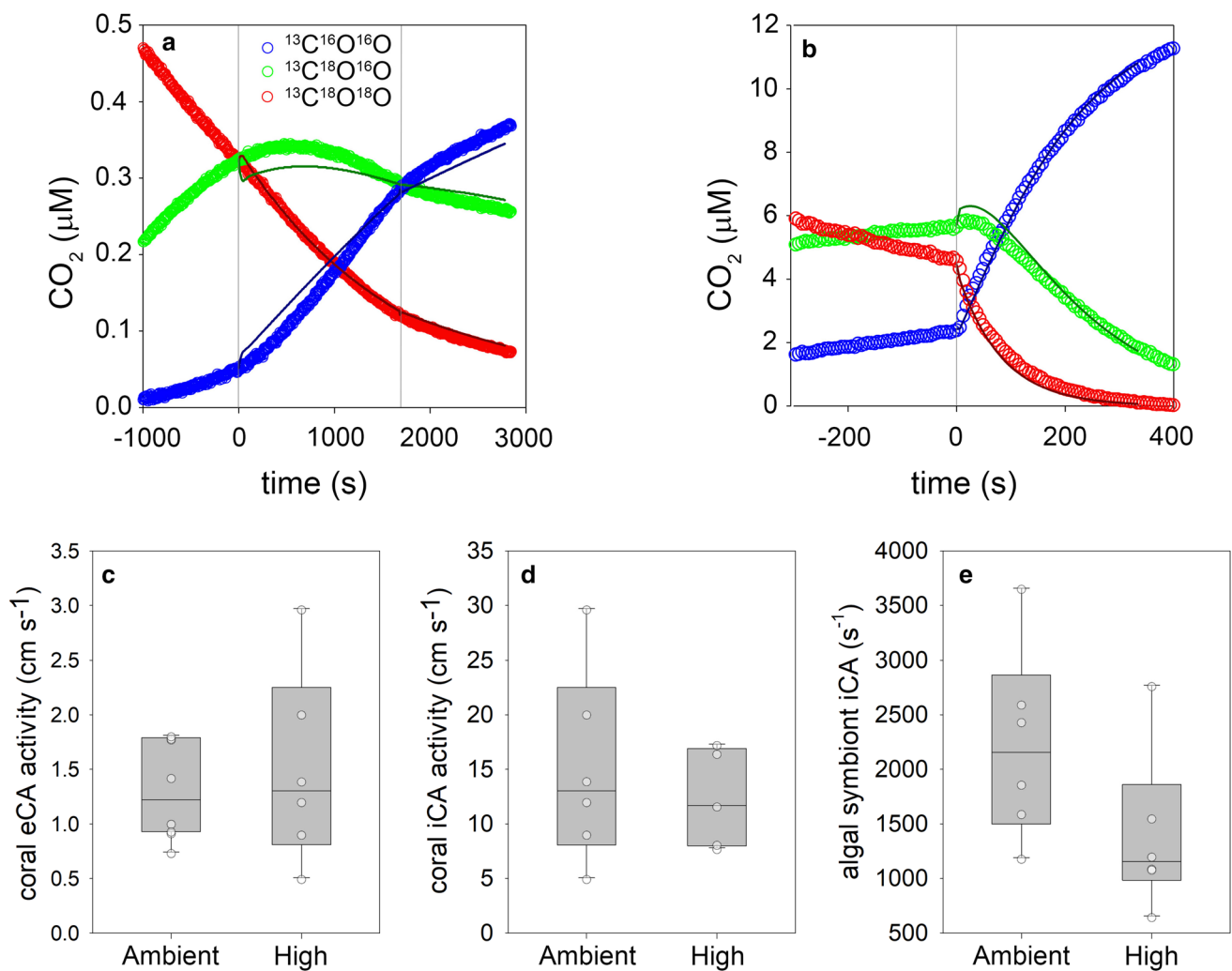
**Fig. 3** Carbonic anhydrase activity for *O. arbuscula* in ambient (490 ppm) and high (840 ppm) $CO_2$ treatments. **a** Sample results from a coral eCA assay illustrating acceleration of $^{18}O$ removal after addition of coral fragment ($t = 0$ s, gray line) and partial slowing of $^{18}O$ removal upon addition of the eCA inhibitor AZ ($t = 1800$ s, gray line). **b** Sample results of a coral iCA assay showing acceleration of $^{18}O$ removal after addition of coral tissue homogenate ($t = 0$ s, gray line). In **a** and **b**, the colored open circles are the isotopologue measurements (blue = $^{13}C^{16}O^{16}O$, green = $^{13}C^{18}O^{16}O$, red = $^{13}C^{18}O^{18}O$) and the solid lines are the model fit to the isotopologue data used to determine CA activities. **c** Coral eCA (*n* per treatment = 5–6), **d** coral iCA (*n* per treatment = 8) activities, **e** algal symbiont iCA activities (*n* per treatment = 5–6). In **c**, **d**, and **e**, the lower and upper bounds of the boxes indicate the 25th and 75th percentiles of the data and the extent of the whiskers indicates the 10th and 90th percentiles. The circles overlying the box plot are the individual data points

**Table 3** Results of nested one-way ANOVAs to assess differences in carbonic anhydrase activities between ambient and high $CO_2$ treatments [*n* per treatment = 5–6 (coral iCA, algal iCA), 8 (coral eCA)]

| Variable | *F* | *df* | *p* value |
| --- | --- | --- | --- |
| Coral iCA | 0.39 | 1, 4 | 0.577 |
| Coral eCA | 0.37 | 1, 4 | 0.567 |
| Algal iCA | 3.16 | 1, 4 | 0.150 |

photosynthetic rates by $39 \pm 16\%$ and by $25 \pm 12\%$ at high $CO_2$, but the differences are not statistically significant (Table 4).

## Discussion

This study sought to examine the physiological mechanisms that enable resilience to OA in the temperate coral *O. arbuscula*. Elevated $CO_2$ concentrations had no statistically significant effects on photosynthetic physiology or carbonic anhydrase activity, a key component of inorganic carbon-processing machinery. These findings suggest that other characteristics such as the ability to maintain calcifying fluid pH or the ability to acquire energy from heterotrophy may be more important for resilience to OA.

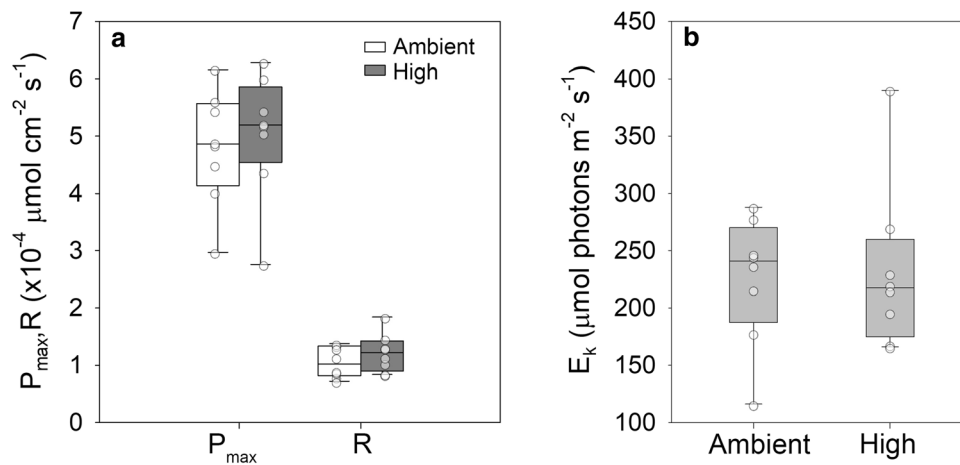The temperate scleractinian coral *O. arbuscula* is an important habitat structuring species in hard bottom

**Fig. 4** Photosynthetic parameters determined from photosynthesis versus irradiance experiments on *O. arbuscula* fragments in ambient (490 ppm) and high (840 ppm) $CO_2$ treatments. **a** The maximal photosynthetic rate at saturating irradiance ($P_{max}$) and the dark respiration rate ($R$), and **b** plots the light saturation parameter ($E_k$).

The lower and upper bounds of the boxes indicate the 25th and 75th percentiles of the data, and the extent of the whiskers indicates the 10th and 90th percentiles. The circles overlying the box plot are the individual data points (*n* per treatment = 8)

**Table 4** Results of nested one-way ANOVAs to assess differences in photophysiological parameters between ambient and high $CO_2$ treatments

| Variable | $F$ | $df$ | $p$ value |
|---|---|---|---|
| $P_{max}$ | 0.02 | 1, 4 | 0.899 |
| $R$ | 0.61 | 1, 4 | 0.479 |
| $E_k$ | 0.31 | 1, 4 | 0.610 |
| $F_v/F_m$ | 0.00 | 1, 4 | 0.985 |
| $\tau_{QA}$ | 1.11 | 1, 4 | 0.352 |
| $\tau_{PQ}$ | 0.00 | 1, 4 | 0.96 |
| AZ-inhib | 2.50 | 1, 4 | 0.189 |

*n* per treatment = 8 ($P_{max}$, $R$, $E_k$), 10–11 ($F_v/F_m$, $\tau_{QA}$, $\tau_{PQ}$, AZ-inhib). AZ-inhib indicates the extent to which acetazolamide inhibited photosynthesis

communities on the continental shelf of the southeastern USA (Gleason et al. 2018). These environments are characterized by dramatic seasonal variation in temperature, light, and $CO_2$ (Xue et al. 2016) requiring broad tolerance in resident organisms, especially sessile species such as *O. arbuscula*. *Oculina arbuscula* is capable of surviving a wide range of temperatures (10–30 °C), light intensities (1–100% of surface irradiance), and $CO_2$ conditions (> 2500 ppm) (Miller 1995; Thornhill et al. 2008; Ries et al. 2010). Although it is clear that this species is capable of tolerating widely varying environmental conditions, the underlying physiological, cellular, and genetic bases of environmental tolerance are generally unknown. The ability of scleractinian corals to withstand high $CO_2$ concentrations has received increasing focus recently with the recognition that OA depresses calcification rates in diverse

calcifying taxa including scleractinian corals, bivalves, and coccolithophores (Ries et al. 2009; Kroeker et al. 2010). In this study, physiological traits that may enable *O. arbuscula*'s demonstrated resilience to OA (Ries et al. 2010, Varnerin et al. 2020) were examined. In particular, this study focused on CA activity, which is involved in inorganic carbon supply for calcification and photosynthesis, and photosynthetic performance. Inorganic carbon supply and photosynthesis may be enhanced by increased $CO_2$ and potentially offset otherwise detrimental effects of OA on calcification.

In our experiments, raising $CO_2$ concentrations from $\sim 500$ to $\sim 850$ ppm had minimal effects on *O. arbuscula* at either the organismal or physiological level. Elevated $CO_2$ had no effect on organismal-level metrics including skeletal growth (calcification) or algal symbiont densities. The lack of effect of $CO_2$ on *O. arbuscula* growth is consistent with several previous studies (Ries et al. 2010; Varnerin et al. 2020), and the principle aim of this work was to assess potential mechanisms underlying this resilience to high $CO_2$. One hypothesis was that high $CO_2$ could stimulate photosynthetic output by *O. arbuscula*'s symbiotic algae providing additional resources that could be used to mitigate the detrimental effect of OA on calcification. However, there was no evidence for this hypothesis as elevated $CO_2$ did not affect photosynthesis versus irradiance characteristics ($P_{max}$, $E_k$, $R$), PSII efficiency ($F_v/F_m$), photosynthetic electron transport properties ($\tau_{QA}$, $\tau_{PQ}$), or algal symbiont densities. Consequently, there is no evidence that increased energetic supplies from symbiotic autotrophs enabled resilience of the coral host.

In contrast to tropical corals, temperate corals likely obtain a higher proportion of their total energy budget from
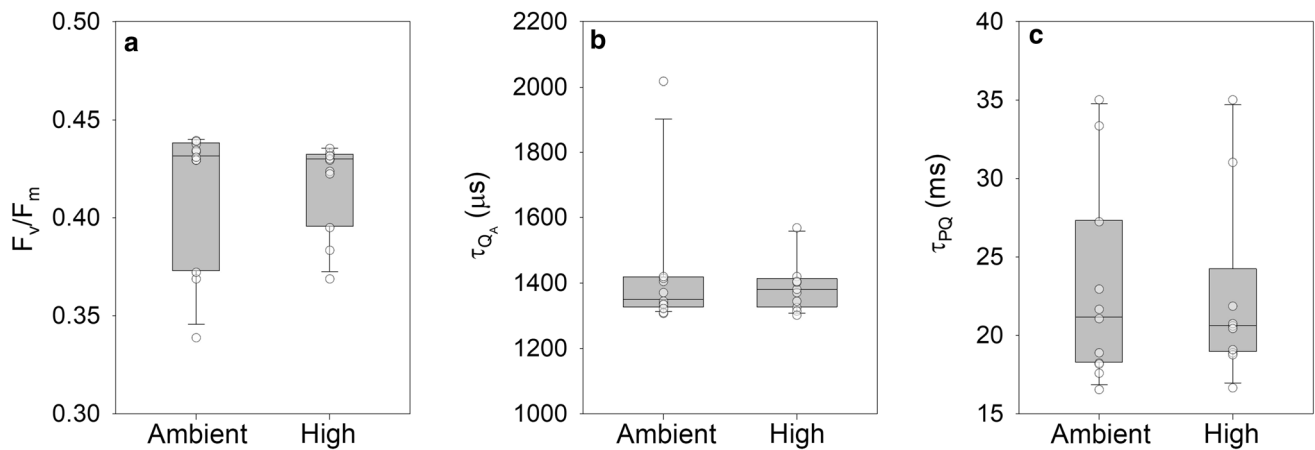
**Fig. 5** Photosynthetic characteristics determined from chlorophyll fluorescence kinetics for *O. arbuscula* in ambient (490 ppm) and high (840 ppm) $CO_2$ treatments. The characteristics measured were **a** the maximal photosynthetic efficiency of PSII ($F_v/F_m$), **b** the turnover time of $Q_A$ ($\tau_{Qa}$), and **c** the turnover time of the plastoquinone pool ($\tau_{PQ}$). The lower and upper bounds of the boxes indicate the 25th and 75th percentiles of the data, and the extent of the whiskers indicates the 10th and 90th percentiles. The circles overlying the box plot are the individual data points (*n* per treatment = 10–11)

heterotrophy and so photosynthetic carbon supplies may be less critical for enabling OA resilience. *Oculina arbuscula* was fed generously three times a week in these experiments, and light levels were low ($\sim$ 50 µmol photons m$^{-2}$ s$^{-1}$) to match in situ conditions (Matterson 2012). Although we did not construct an energy budget, these considerations suggest that heterotrophy may have been a significant energy source. In tropical corals, heterotrophy helps corals withstand stressors such as OA (Edmunds 2011; Towle et al. 2015) and bleaching (Grottoli et al. 2006). Heterotrophy has been shown to mitigate the effects of temperature stress on *O. arbuscula* specifically (Aichelman et al. 2016) and could reasonably be expected to help this species withstand OA as well. Increased heterotrophy is linked to greater energy availability and reserves through lipid accumulation under both temperature and $CO_2$ stress (Grottoli et al. 2004, 2006; Towle et al. 2015).

A second possible source of resilience to high $CO_2$ lies in the inorganic carbon-processing system that delivers inorganic carbon for calcification and photosynthesis. Corals import $CO_2$ and bicarbonate from the external environment and recycle-respired $CO_2$ to support photosynthesis and calcification (Tambutte et al. 2011; Tansik et al. 2015). These inorganic carbon sources are transported through tissues layers by both active and diffusive mechanisms, the details of which have yet to be fully resolved. CAs serve critical roles in carbon routing by interconverting $CO_2$ and bicarbonate (Moya et al. 2008; Bertucci et al. 2011). To gain insight into potential shifts in inorganic processing at high $CO_2$, *O. arbuscula*'s eCA and iCA activities were measured as a proxy for inorganic processing capacity (Bertucci et al. 2013; Hopkinson et al.

2015). However, no significant differences in either of these parameters were detected, suggesting that no major rearrangements in carbon processing occurred, with the caveat that these measurements represent bulk CA activities and do not resolve the activities of specific isoforms with differing functional roles. Maintenance of high CA activity at elevated $CO_2$ could be a sign of OA resilience since CA gene expression is often, though not always, down-regulated at high $CO_2$ in tropical corals suggesting a reduced capacity for carbon processing when subject to OA (Moya et al. 2012; Kaniewska et al. 2015). Previous physiological and transcriptomic work on tropical corals has indicated that the ability to maintain a high pH in the calcifying fluid at high $CO_2$ confers resilience to OA (McCulloch et al. 2012; Venn et al. 2013; Davies et al. 2016; Strader et al. 2020), and there is some evidence for this in temperate corals as well (Trotter et al. 2011). Characteristics of the calcifying fluid were not assessed in this study, and so it may be that maintaining a high calcifying fluid pH (McCulloch et al. 2012), likely through enhanced proton export, or additional calcium import (DeCarlo et al. 2018), is critical to OA resilience in temperate corals as well.

There was substantial variance in many traits (algal symbiont density, CA activity) within treatments that limited our ability to detect any potentially moderate effects of OA on coral physiology. This individual variation may have both environmental and genetic components. Though the specimens had been in aquaria with controlled environmental conditions for approximately 10 weeks at the time of harvest, acclimation in corals to new conditions can take months (Gates and Edmunds 1999; Mayfield et al. 2018). Consequently, some of the individual variation

could reflect residual effects of differences in environmental conditions in which parent colonies grew. Genetic differences can also lead to variability in physiological responses among individuals exposed to similar conditions, as has been well documented in coral response to temperature change (Dixon et al. 2015; Fuller et al. 2020). This genotype by environment interaction can be partially mitigated by ensuring that replicates of a single genotype are distributed among treatments. However, permit restrictions on the size and number of *O. arbuscula* colonies that could be collected precluded taking coral samples that were large enough to be subdivided and dispersed in both OA treatments.

While no major changes in CA activity or photosynthetic properties were detected in *O. arbuscula*, another possibility is that *O. arbuscula*'s physiology is exceptional in some way, even at ambient $CO_2$, preventing harmful effects of OA. Comparing *O. arbuscula*'s photosynthetic physiology with those of tropical corals, as compiled in Sawall and Hochberg (2018), revealed very similar characteristics between the two groups. Maximal photosynthetic rates of *O. arbuscula* ($\sim 4.5 \times 10^{-4}$ µmol $O_2$ cm$^{-2}$ s$^{-1}$) are nearly identical to average tropical rates ($4.6 \pm 2.3 \times 10^{-4}$ µmol $O_2$ cm$^{-2}$ s$^{-1}$, average $\pm$ standard deviation). The light saturation parameter ($E_k$) varies more widely in tropical corals since it is highly dependent on environmental light conditions, but *O. arbuscula*'s $E_k$ under our experimental conditions ($229 \pm 62$ µmol photons m$^{-2}$ s$^{-1}$) is well within the typical range of tropical corals ($186 \pm 100$ µmol photons m$^{-2}$ s$^{-1}$, average $\pm$ standard deviation). This comparison suggests that *O. arbuscula*'s photosynthetic potential is similar to that of tropical corals, which are able to support most of their energetic needs through photosynthesis (Muscatine et al. 1981; Edmunds and Davies 1986). The combination of substantial photosynthetic and heterotrophic energy sources in this experiment may have provided sufficient energy to counteract negative effects of OA, as noted above. Comparisons of *O. arbuscula*'s CA activities with the few previous quantitative CA activity measurements also indicated that these traits are similar in tropical coral and *O. arbuscula*. eCA activities in three tropical corals, *Orbicella faveolata*, *Porites astreoides,* and *Siderastrea radians*, ranged between maximum values of $\sim 6$ cm s$^{-1}$ in *O. faveolata* down to $\sim 0.1$ in *P. astreoides* (Tansik et al. 2015), and *O. arbuscula* averaged $\sim 1$ cm s$^{-1}$. iCA activities in the same three tropical corals were in the range of 4–12 cm s$^{-1}$ (Hopkinson et al. 2015), and *O. arbuscula* averaged $\sim 14$ cm s$^{-1}$, on the high end but not dramatically different from tropical corals. Notably, all of these tropical corals have impaired growth under moderate OA conditions (Okazaki et al. 2013; Langdon et al. 2018; Bove et al. 2019), suggesting CA activity, as a proxy for inorganic processing capacity, is not a good indicator of OA resilience.

Like many other temperate (Rodolfo-Metalpa et al. 2010) and slow-growing tropical corals (Comeau et al. 2014), *O. arbuscula*'s growth and calcification rates are resilient to OA, both in adult (Ries et al. 2010) and in juvenile (Varnerin et al. 2020) life stages. Here, the potential roles of changes in photosynthetic physiology and inorganic carbon processing in conferring resilience were assessed. There was no evidence that increased photosynthetic production at higher $CO_2$ provided additional energy to counteract OA, perhaps because the coral host regulates $CO_2$ supply to their algal symbionts (Tansik et al. 2017). Similarly, carbonic anhydrase activity of the coral was unaltered by elevated $CO_2$ concentrations though this does suggest that inorganic carbon flows to photosynthesis and calcification are maintained at high $CO_2$ in contrast to several tropical corals that down-regulate CA under OA conditions (Moya et al. 2012; Kaniewska et al. 2015). Explanations for why temperate and slow-growing corals are resilient to OA may lie in how the chemistry of the calcifying fluid is regulated (McCulloch et al. 2012; Strader et al. 2020), increased reliance on heterotrophy, or simply reflect the fact that slower growing corals invest less energy in skeletal formation (Comeau et al. 2014).

**Compliance with ethical standards**

**Conflict of interest** On behalf of all authors, the corresponding author states that there is no conflict of interest.

# References

Aichelman HE, Townsend JE, Courtney TA, Baumann JH, Davies SW, Castillo KD (2016) Heterotrophy mitigates the response of the temperate coral Oculina arbuscula to temperature stress. Ecol Evol 6:6758–6769

Anthony KRN, Kline DI, Diaz-Pulido G, Dove S, Hoegh-Guldberg O (2008) Ocean acidification causes bleaching and productivity loss in coral reef builders. Proceedings of the National Academy of Sciences of the United States of America 105:17442–17446

Bertucci A, Tambutte S, Supuran CT, Allemand D, Zoccola D (2011) A New Coral Carbonic Anhydrase in *Stylophora pistillata*. Mar Biotechnol 13:992–1002

Bertucci A, Moya A, Tambutte S, Allemand D, Supuran CT, Zoccola D (2013) Carbonic anhydrases in anthozoan corals-A review. Bioorganic & Medicinal Chemistry 21:1437–1450

Bove CB, Ries JB, Davies SW, Westfield IT, Umbanhowar J, Castillo KD (2019) Common Caribbean corals exhibit highly variable responses to future acidification and warming. Proceedings of the Royal Society B-Biological Sciences 286:9

Cai WJ, Ma YN, Hopkinson BM, Grottoli AG, Warner ME, Ding Q, Hu XP, Yuan XC, Schoepf V, Xu H, Han CH, Melman TF, Hoadley KD, Pettay DT, Matsui Y, Baumann JH, Levas S, Ying Y, Wang YC (2016) Microelectrode characterization of coral daytime interior pH and carbonate chemistry. Nature Communications 7:8

Chan NCS, Connolly SR (2013) Sensitivity of coral calcification to ocean acidification: a meta-analysis. Global Change Biology 19:282–290

Cohen AL, McConnaughey TA (2003) Geochemical perspectives on coral mineralization. In: Dove PM, DeYoreo JJ, Weiner S (eds) Biomineralization. Mineralogical Soc Amer, Chantilly, pp 151–187

Comeau S, Carpenter RC, Edmunds PJ (2013) Coral reef calcifiers buffer their response to ocean acidification using both bicarbonate and carbonate. Proceedings of the Royal Society B-Biological Sciences 280:8

Comeau S, Edmunds PJ, Spindel NB, Carpenter RC (2014) Fast coral reef calcifiers are more sensitive to ocean acidification in short-term laboratory incubations. Limnology and Oceanography 59:1081–1091

Comeau S, Cornwall CE, DeCarlo TM, Krieger E, McCulloch MT (2018) Similar controls on calcification under ocean acidification across unrelated coral reef taxa. Global Change Biology 24:4857–4868

Davies SW, Marchetti A, Ries JB, Castillo KD (2016) Thermal and $pCO_2$ Stress Elicit Divergent Transcriptomic Responses in a Resilient Coral. Frontiers in Marine Science 3:15

DeCarlo TM, Comeau S, Cornwall CE, McCulloch MT (2018) Coral resistance to ocean acidification linked to increased calcium at the site of calcification. Proceedings of the Royal Society B-Biological Sciences 285:7

Dickson AG, Goyet C (1994) DOE handbook of methods for the analysis of the various parameters of the carbon dioxide system in sea water. Version 2. ORNL/CDIAC-74

Dixon GB, Davies SW, Aglyamova GA, Meyer E, Bay LK, Matz MV (2015) Genomic determinants of coral heat tolerance across latitudes. Science 348:1460–1462

Doney SC, Fabry VJ, Feely RA, Kleypas JA (2009) Ocean Acidification: The Other $CO_2$ Problem. Annual Review of Marine Science 1:169–192

Drake JL, Mass T, Stolarski J, Von Euw S, van de Schootbrugge B, Falkowski PG (2020) How corals made rocks through the ages. Global Change Biology 26:31–53

Edmunds PJ (2011) Zooplanktivory ameliorates the effects of ocean acidification on the reef coral *Porites* spp. Limnology and Oceanography 56:2402–2410

Edmunds PJ, Davies PS (1986) An energy budget for *Porites porites* (Scleractinia). Mar Biol 92:339–347

Edmunds PJ, Comeau S, Lantz C, Andersson A, Briggs C, Cohen A, Gattuso JP, Grady JM, Gross K, Johnson M, Muller EB, Ries JB, Tambutte S, Tambutte E, Venn A, Carpenter RC (2016) Integrating the Effects of Ocean Acidification across Functional Scales on Tropical Coral Reefs. Bioscience 66:350–362

Fuller ZL, Mocellin VJL, Morris LA, Cantin N, Shepherd J, Sarre L, Peng J, Liao Y, Pickrell J, Andolfatto P, Matz M, Bay LK, Przeworski M (2020) Population genetics of the coral Acropora millepora: Toward genomic prediction of bleaching. Science 369:268–277

Furla P, Galgani I, Durand I, Allemand D (2000) Sources and mechanisms of inorganic carbon transport for coral calcification and photosynthesis. J Exp Biol 203:3445–3457

Gates RD, Edmunds PJ (1999) The physiological mechanisms of acclimatization in tropical reef corals. Am Zool 39:30–43

Gleason DF, Harbin LR, Divine LM, Matterson KO (2018) The role of larval supply and competition in controlling recruitment of the temperate coral *Oculina arbuscula*. Journal of Experimental Marine Biology and Ecology 506:107–114

Grottoli AG, Rodrigues LJ, Juarez C (2004) Lipids and stable carbon isotopes in two species of Hawaiian corals, Porites compressa and Montipora verrucosa, following a bleaching event. Marine Biology 3:621–631

Grottoli AG, Rodrigues LJ, Palardy JE (2006) Heterotrophic plasticity and resilience in bleached corals. Nature 440:1186–1189

Gruber N, Clement D, Carter BR, Feely RA, van Heuven S, Hoppema M, Ishii M, Key RM, Kozyr A, Lauvset SK, Lo Monaco C, Mathis JT, Murata A, Olsen A, Perez FF, Sabine CL, Tanhua T, Wanninkhof R (2019) The oceanic sink for anthropogenic $CO_2$ from 1994 to 2007. Science 363:1193-+

Hoadley KD, Pettay DT, Grottoli AG, Cai WJ, Melman TF, Schoepf V, Hu XP, Li Q, Xu H, Wang YC, Matsui Y, Baumann JH, Warner ME (2015) Physiological response to elevated temperature and $pCO_2$ varies across four Pacific coral species: Understanding the unique host plus symbiont response. Sci Rep 5:15

Hofmann GE, Barry JP, Edmunds PJ, Gates RD, Hutchins DA, Klinger T, Sewell MA (2010) The Effect of Ocean Acidification on Calcifying Organisms in Marine Ecosystems: An Organism-to-Ecosystem Perspective. In: Futuyma DJ, Shafer HB, Simberloff D (eds) Annual Review of Ecology, Evolution, and Systematics, Vol 41. Annual Reviews, Palo Alto, pp 127–147

Hopkinson BM, Dupont CL, Allen AE, Morel FMM (2011) Efficiency of the $CO_2$-concentrating mechanism of diatoms. Proceedings of the National Academy of Sciences of the United States of America 108:3830–3837

Hopkinson BM, Meile C, Shen C (2013) Quantification of extracellular carbonic anhydrase activity in two marine diatoms and investigation of its role. Plant Physiology 162:1142–1152

Hopkinson BM, Tansik AL, Fitt WK (2015) High internal carbonic anhydrase activity in the tissue of scleractinian corals is sufficient to support proposed roles in photosynthesis and calcification. J Exp Biol 218:2039–2048

Hughes TP, Anderson KD, Connolly SR, Heron SF, Kerry JT, Lough JM, Baird AH, Baum JK, Berumen ML, Bridge TC, Claar DC, Eakin CM, Gilmour JP, Graham NAJ, Harrison H, Hobbs JPA, Hoey AS, Hoogenboom M, Lowe RJ, McCulloch MT, Pandolfi JM, Pratchett M, Schoepf V, Torda G, Wilson SK (2018) Spatial and temporal patterns of mass bleaching of corals in the Anthropocene. Science 359:80–83

IPCC, 2014: Climate Change 2014: Synthesis Report. Contribution of Working Groups I, II and III to the Fifth Assessment Report of the Intergovernmental Panel on Climate Change [Core Writing Team, R.K. Pachauri and L.A. Meyer (eds.)]. IPCC, Geneva, Switzerland, 151 pp

Jokiel PL, Maragos JE, Franzisket L (1978) Coral growth: buoyant weight technique. In: Stoddart DR, Johannes RE (eds) Coral Reefs: research methods. UNESCO, Paris, France

Kaniewska P, Chan CKK, Kline D, Ling EYS, Rosic N, Edwards D, Hoegh-Guldberg O, Dove S (2015) Transcriptomic changes in coral holobionts provide insights into physiological challenges of future climate and ocean change. PloSone 10:e0139223

Koch M, Bowes G, Ross C, Zhang XH (2013) Climate change and ocean acidification effects on seagrasses and marine macroalgae. Global Change Biology 19:103–132

Kolber ZS, Prasil O, Falkowski PG (1998) Measurements of variable chlorophyll fluorescence using fast repetition rate techniques: defining methodology and experimental protocols. Biochim Biophys Acta-Bioenerg 1367:88–106

Kroeker KJ, Kordas RL, Crim RN, Singh GG (2010) Meta-analysis reveals negative yet variable effects of ocean acidification on marine organisms. Ecology Letters 13:1419–1434

Kroeker KJ, Kordas RL, Crim R, Hendriks IE, Ramajo L, Singh GS, Duarte CM, Gattuso JP (2013) Impacts of ocean acidification on marine organisms: quantifying sensitivities and interaction with warming. Global Change Biology 19:1884–1896

LaJeunesse TC, Parkinson JE, Gabrielson PW, Jeong HJ, Reimer JD, Voolstra CR, Santos SR (2018) Systematic Revision of Symbiodiniaceae Highlights the Antiquity and Diversity of Coral Endosymbionts. Curr Biol 28:2570–2580

Langdon C, Atkinson MJ (2005) Effect of elevated $pCO_2$ on photosynthesis and calcification of corals and interactions with seasonal change in temperature/irradiance and nutrient enrichment. J Geophys Res-Oceans 110

Langdon C, Albright R, Baker AC, Jones P (2018) Two threatened Caribbean coral species have contrasting responses to combined temperature and acidification stress. Limnology and Oceanography 63:2450–2464

Leydet KP, Hellberg ME (2016) Discordant coral-symbiont structuring: factors shaping geographical variation of Symbiodinium communities in a facultative zooxanthellate coral genus, Oculina. Coral Reefs 35:583–595

Mackey KRM, Morris JJ, Morel FMM, Kranz SA (2015) Response of Photosynthesis to Ocean Acidification. Oceanography 28:74–91

Marsh JA (1970) Primary Productivity of reef-building calcareous red algae. Ecology 51:255–263

Matterson K (2012) Microscale variation in light intensity and its effects on growth of juveniles of the temperate coral, Oculina arbuscula. Georgia Southern University, p 71

Mayfield AB, Chen YJ, Lu CY, Chen CS (2018) The proteomic response of the reef coral Pocillopora acuta to experimentally elevated temperatures. PLoS One 13:24

McCulloch M, Falter J, Trotter J, Montagna P (2012) Coral resilience to ocean acidification and global warming through pH up-regulation. Nat Clim Chang 2:623–633

Miller MW (1995) Growth of a temperate coral - effects of temperature, light, depth, and heterotrophy. Mar Ecol-Prog Ser 122:217–225

Moya A, Tambutte S, Bertucci A, Tambutte E, Lotto S, Vullo D, Supuran CT, Allemand D, Zoccola D (2008) Carbonic anhydrase in the scleractinian coral Stylophora pistillata - Characterization, localization, and role in biomineralization. Journal of Biological Chemistry 283:25475–25484

Moya A, Huisman L, Ball EE, Hayward DC, Grasso LC, Chua CM, Woo HN, Gattuso JP, Foret S, Miller DJ (2012) Whole Transcriptome Analysis of the Coral Acropora millepora Reveals Complex Responses to $CO_2$-driven Acidification during the Initiation of Calcification. Molecular Ecology 21:2440–2454

Muller EM, Sartor C, Alcaraz NI, van Woesik R (2020) Spatial Epidemiology of the Stony-Coral-Tissue-Loss Disease in Florida. Frontiers in Marine Science 7:11. https://doi.org/10.3389/fmars.2020.00163

Muscatine L, McCloskey LR, Marian RE (1981) Estimating the daily contribution of carbon from zooxanthellae to coral animal respiration. Limnology and Oceanography 26:601–611

Okazaki RR, Swart PK, Langdon C (2013) Stress-tolerant corals of Florida Bay are vulnerable to ocean acidification. Coral Reefs 32:671–682

Price NM, Harrison GI, Hering JG, Hudson RJ, Nirel PMV, Palenik B, Morel FMM (1988) Preparation and chemistry of the artificial algal culture medium Aquil. Biological Oceanography 6:443–462

Riebesell U, Zondervan I, Rost B, Tortell PD, Zeebe RE, Morel FMM (2000) Reduced calcification of marine plankton in response to increased atmospheric $CO_2$. Nature 407:364–367

Riebesell U, Fabry VJ, Hansson L, Gattuso JP (2011) Guide to best practices for ocean acidification research and data reporting. European Commission

Ries JB, Cohen AL, McCorkle DC (2009) Marine calcifiers exhibit mixed responses to $CO_2$-induced ocean acidification. Geology 37:1131–1134

Ries JB, Cohen AL, McCorkle DC (2010) A nonlinear calcification response to $CO_2$-induced ocean acidification by the coral Oculina arbuscula. Coral Reefs 29:661–674

Rodolfo-Metalpa R, Martin S, Ferrier-Pages C, Gattuso JP (2010) Response of the temperate coral Cladocora caespitosa to mid- and long-term exposure to $pCO_2$ and temperature levels projected for the year 2100 AD. Biogeosciences 7:289–300

Sawall Y, Hochberg EJ (2018) Diel versus time-integrated (daily) photosynthesis and irradiance relationships of coral reef organisms and communities. PLoS One 13:13

Sevilgen DS, Venn AA, Hu MY, Tambutte E, de Beer D, Planas-Bielsa V, Tambutte S (2019) Full in vivo characterization of carbonate chemistry at the site of calcification in corals. Sci Adv 5:9

Silverman D (1982) Carbonic anhydrase: oxygen-18 exchange catalyzed by an enzyme with rate-contributing proton-transfer steps. Methods in enzymology 87:732–752

Stachowicz JJ, Hay ME (1999) Mutualism and coral persistence: The role of herbivore resistance to algal chemical defense. Ecology 80:2085–2101

Strader ME, Wong JM, Hoffman GE (2020) Ocean acidification promotes broad transcriptomic responses in marine metazoans: a literature survey. Frontiers in Zoology 17

Tambutte S, Holcomb M, Ferrier-Pages C, Reynaud S, Tambutte E, Zoccola D, Allemand D (2011) Coral biomineralization: From the gene to the environment. Journal of Experimental Marine Biology and Ecology 408:58–78

Tansik AL, Fitt WK, Hopkinson BM (2015) $CO_2$ uptake facilitated by an extracellular carbon anhydrase is critical for photosynthesis in symbiotic corals. Coral Reefs 34:703–713

Tansik AL, Fitt WK, Hopkinson BM (2017) Inorganic carbon is scarce for symbionts in scleractinian corals. Limnology and Oceanography 62:2045–2055

Thornhill DJ, Kemp DW, Bruns BU, Fitt WK, Schmidt GW (2008) Correspondence between cold tolerance and temperate biogeography in a western atlantic Symbiodinium (Dinophyta) lineage. Journal of Phycology 44:1126–1135

Thrane JE, Kyle M, Striebel M, Hannde S, Grung M, Rohrlack T, Andersen T (2015) Spectrophotometric Analysis of Pigments: A Critical Assessment of a High-Throughput Method for Analysis of Algal Pigment Mixtures by Spectral Deconvolution. PLoS One 10:e0137645

Tortell PD, Payne CD, Li YY, Trimborn S, Rost B, Smith WO, Riesselman C, Dunbar RB, Sedwick P, DiTullio GR (2008) $CO_2$ sensitivity of Southern Ocean phytoplankton. Geophys Res Lett 35

Towle EK, Enochs IC, Langdon C (2015) Threatened Caribbean Coral Is Able to Mitigate the Adverse Effects of Ocean Acidification on Calcification by Increasing Feeding Rate. PLoS One 10:17

Trotter J, Montagna P, McCulloch M, Silenzi S, Reynaud S, Mortimer G, Martin S, Ferrier-Pages C, Gattuso J-P, Rodolfo-Metalpa R (2011) Quantifying the pH 'vital effect' in the temperate zooxanthellate coral Cladocora caespitosa: Validation of the boron seawater pH proxy. Earth Planet Sci Lett 303:163–173

Varnerin BV, Hopkinson BM, Gleason DF (2020) Recruits of the temperate coral *Oculina arbuscula* mimic adults in their resilience to ocean acidification. Mar Ecol-Prog Ser 636:63–75

Venn AA, Tambutte E, Holcomb M, Laurent J, Allemand D, Tambutte S (2013) Impact of seawater acidification on pH at the tissue-skeleton interface and calcification in reef corals. Proceedings of the National Academy of Sciences of the United States of America 110:1634–1639

Xue L, Cai WJ, Hu XP, Sabine C, Jones S, Sutton AJ, Jiang LQ, Reimer JJ (2016) Sea surface carbon dioxide at the Georgia time series site (2006-2007): Air-sea flux and controlling processes. Prog Oceanogr 140:14–26

Zaneveld JR, Burkepile DE, Shantz AA, Pritchard CE, McMinds R, Payet JP, Welsh R, Correa AMS, Lemoine NP, Rosales S, Fuchs C, Maynard JA, Thurber RV (2016) Overfishing and nutrient pollution interact with temperature to disrupt coral reefs down to microbial scales. Nature Communications 7:12

Zhang HN, Byrne RH (1996) Spectrophotometric pH measurements of surface seawater at in situ conditions: Absorbance and protonation behavior of thymol blue. Mar Chem 52:17–25